

Manual Control Adaptation to Variations in Short-Period Natural Frequency and Damping

Fasiello, Simone; Lu, T.; Pool, Daan; van Paassen, Rene

DOI

[10.2514/6.2019-1230](https://doi.org/10.2514/6.2019-1230)

Publication date

2019

Document Version

Final published version

Published in

AIAA Scitech 2019 Forum

Citation (APA)

Fasiello, S., Lu, T., Pool, D., & van Paassen, R. (2019). Manual Control Adaptation to Variations in Short-Period Natural Frequency and Damping. In *AIAA Scitech 2019 Forum: 7-11 January 2019, San Diego, California, USA* Article AIAA 2019-1230 <https://doi.org/10.2514/6.2019-1230>

Important note

To cite this publication, please use the final published version (if applicable). Please check the document version above.

Copyright

Other than for strictly personal use, it is not permitted to download, forward or distribute the text or part of it, without the consent of the author(s) and/or copyright holder(s), unless the work is under an open content license such as Creative Commons.

Takedown policy

Please contact us and provide details if you believe this document breaches copyrights. We will remove access to the work immediately and investigate your claim.



Manual Control Adaptation to Variations in Short-Period Natural Frequency and Damping

S. Fasiello,*
Delft University of Technology
Delft, The Netherlands
and
University of Liverpool
Liverpool, United Kingdom
and
Politecnico di Milano
Milano, Italy

T. Lu,[†] D.M. Pool,[‡] and M.M. van Paassen[§]
Delft University of Technology
Delft, The Netherlands

This paper presents the results of a human-in-the-loop experiment performed to investigate the effects of variations in aircraft short-period mode characteristics on human operators' manual control behavior. In the experiment, 15 participants performed a tracking task for a factorial variation in both short-period mode natural frequency (five settings) and damping ratio (three settings). The baseline aircraft dynamics were those of a Cessna Citation aircraft, as used in a number of previous experiments, and the variations in short-period dynamics were chosen to span a range of interest with respect to available handling qualities criteria and Maximum Unnoticed Added Dynamics (MUAD) envelopes. To objectively quantify the induced adaptation of manual control behavior, human operator models were fitted to the collected tracking data. In addition to these control behavior measures also subjective ratings of the noticeability of differences with respect to the baseline aircraft were collected. Overall, the results show consistent adaptation of manual control behavior to variations in both short-period parameters and a worsening of task performance with decreased short-period natural frequency and decreased damping ratio settings. In spite of inconsistencies in the subjective rating data, the overall objective adaptation of manual control dynamics correlates with the subjective noticeability ratings, as well as correspondence of the tested configurations with available MUAD envelopes.

I. Introduction

The concepts of “maximum unnoticed added dynamics” (MUAD)^{1–3} or “maximum allowable errors” (AE)⁴ are traditionally used in studies of aircraft handling qualities,^{5–13} to formalize the human pilot's sensitivity to the specific dynamics of his controlled aircraft. This sensitivity is generally expressed as a frequency-domain (MUAD or AE) envelope within which any added dynamics (e.g., augmented systems, system failures) to the original aircraft dynamics will remain unnoticed by the pilot. The envelope boundaries are derived from subjective evaluations of a large number of added dynamics in a challenging manual control task.^{1–3} Currently, detailed knowledge on when changes in controlled dynamics become noticeable for human pilots in manual control of their aircraft, is highly relevant as a benchmark for the required accuracy of aircraft dynamics models used in flight simulators.

It is widely known that in manual control tasks human controllers adapt and optimize their control behaviour to the dynamics they control.^{14,15} Furthermore, this adaptation and optimization of pilots' control behavior can be objectively measured using state-of-art manual control identification and modeling methods.^{16–18} To overcome some of the limitations of relying on subjective impressions of noticeability in the development of criteria meant to reflect human sensitivity to changes in controlled aircraft dynamics, at our group we are pursuing a “cybernetic” approach to

*Ph.D. student, University of Liverpool and Politecnico di Milano, School of Engineering, Brownlow Hill, L69 3GH, Liverpool, UK; s.fasiello@liverpool.ac.uk. Student Member AIAA.

[†]Ph.D. student, Control and Simulation Division, Faculty of Aerospace Engineering, P.O. Box 5058, 2600GB Delft, The Netherlands; t.lu-3@tudelft.nl

[‡]Assistant Professor, Control and Simulation Division, Faculty of Aerospace Engineering, P.O. Box 5058, 2600GB Delft, The Netherlands; d.m.pool@tudelft.nl. Member AIAA.

[§]Associate Professor, Control and Simulation Division, Faculty of Aerospace Engineering, P.O. Box 5058, 2600GB Delft, The Netherlands; m.m.vanpaassen@tudelft.nl. Member AIAA.

this problem, based on (objectively measurable) control behavior adaptations in tracking tasks.^{18–20} Such a cybernetic, objective and control behavior-based, analysis of human sensitivity of variations in controlled dynamics can provide quantitative verification and additional insight into the concept of MUAD and AE envelopes.

While in earlier work we have focused explicitly on quantifying induced behavioral adaptation due to *added (dipole) dynamics* for varying dipole parameter settings,^{19,20} the current paper applies the same methodology for considering allowable variations in the key parameters of controlled *baseline aircraft dynamics*. The current investigation focuses on manual control behavior in a pitch tracking task also considered in a number of earlier experiments,^{19,21–24} where a low-order approximation of the elevator-to-pitch dynamics of a Cessna Citation aircraft are controlled. This paper describes a human-in-the-loop experiment with 15 participants performed to measure manual control adaptation for a range of parameter settings of the two parameters characterizing the short-period mode, i.e., the short-period natural frequency and damping ratio. For quantitative analysis of behavioral changes, tracking performance and control activity metrics are used, as well as explicit human control model parameters estimated with state-of-the-art identification methods.²⁵ Furthermore, a methodology is proposed and tested for estimating the overall “objective” noticeability of changes in the controlled dynamics from observed variations in a subset of key control behavioral metrics.

This paper is structured as follows. First, Section II describes the human-in-the-loop experiment setup and procedures. The experiment results, consisting of both subjective ratings and objective control behavior measures, are presented in Section III. The paper ends with a discussion and conclusions.

II. Methods

II.A. Control task

Fig. 1 shows a block diagram of the pitch attitude control task considered in the experiment, which is equivalent to the tasks from earlier experiments.^{19,21,22} In this task, the human operator’s goal is to make the pitch attitude θ of the controlled system ($H_c(s)$) follow a pre-defined target forcing function signal f_t as accurately as possible. The task is compensatory, as only the tracking error e – i.e., the difference between f_t and θ – is shown to the human operator. In compensatory tasks, human operator control dynamics are quasi-linear^{14,15} and can be modeled with a linear response function $H_p(s)$ combined with a remnant signal n that accounts for operator-injected noise and other nonlinear contributions to the operator’s control inputs u . All signals in Fig. 1 have the unit of degrees in this paper.

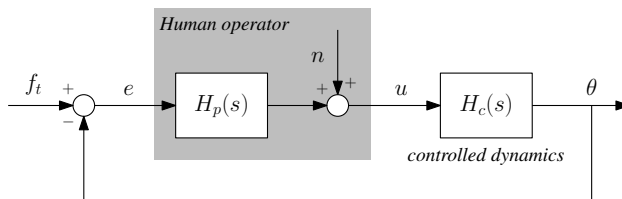


Figure 1. Block diagram of the closed-loop aircraft pitch control task

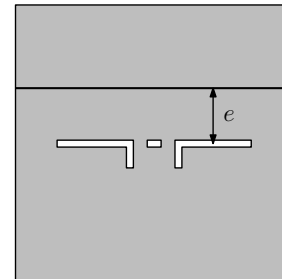


Figure 2. Compensatory display.

In the control task, compensatory display shown in Fig. 2 was used to present participants with the tracking error e . This display is identical to that used in previous experiments.^{19,23} The tracking error is displayed as the displacement of a (yellow) target line with respect to a fixed (white) aircraft symbol, on a contrasting (sky blue) background. The display had an inside-out representation, i.e., correcting the error shown in Fig. 2 requires a pitch-up (aft) input.

II.B. Controlled Dynamics

One of the key factors that affects human operators’ control in compensatory tracking is the dynamics of the controlled system, $H_c(s)$ in Fig. 1. For example, as formalized in the well-known *crossover model*,^{14,15} human operators are known to explicitly adapt their own control dynamics $H_p(s)$ to those of the controlled system to achieve satisfactory characteristics of the combined open-loop system, $H_{ol}(s) = H_p(s)H_c(s)$. The goal of this experiment was to investigate human operators’ sensitivity and adaptation to parameter variations in controlled dynamics of the form:

$$H_c(s) = \frac{K_c (T_{\theta_2} s + 1)}{s \left(\frac{s^2}{\omega_{sp}^2} + \frac{2\zeta_{sp}s}{\omega_{sp}} + 1 \right)} \quad (1)$$

Eq. (1) represents a typical low-order fixed-airspeed approximation of aircraft pitch attitude dynamics,^{5,26,27} as also considered in a number of recent tracking experiments.^{21–24} Note that the units of the in- and output signals of Eq. (1) – u and θ , respectively, see Fig. 1 – are both deg.

In Eq. (1), K_c represents the static control gain, T_{θ_2} is the short-period lead time constant, and ω_{sp} and ζ_{sp} are the short-period mode's natural frequency and damping ratio, respectively. To tie in with previous experiments,^{21,22} the parameters for the baseline controlled dynamics in this paper were set to $K_c = 0.4$, $T_{\theta_2} = 1.0$ s, $\omega_{sp} = 2.75$ rad/s, and $\zeta_{sp} = 0.5$. These controlled dynamics are representative for a Cessna Citation I Ce500 flying at 10,000 ft (3048 m) at an airspeed of 160 kts (87 m/s). Note that in these parameter values, the separate stick gain considered in Refs. 21 and 22 is accounted for. Fig. 3 shows the frequency response (Bode diagram) of these baseline controlled dynamics.

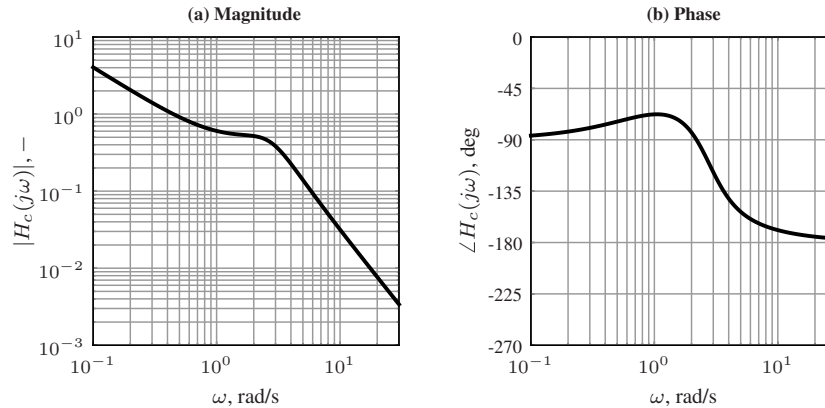


Figure 3. Baseline controlled dynamics frequency response.

II.C. Forcing Function

The target signal f_t inserted in the closed-loop of our system was a quasi-random multisine signal consisting of $N_t = 10$ sinusoids, equivalent to the signal used in earlier experiments.^{19,21}

$$f_t(t) = \sum_{k=1}^{N_t} A_t[k] \sin(\omega_t[k]t + \phi_t[k]) \quad (2)$$

In Eq. (2), $\omega_t[k]$, $A_t[k]$ and $\phi_t[k]$ indicate the frequency, amplitude, and phase of the k^{th} sinusoid in f_t . To enable identification of human control dynamics with frequency-domain methods, the sinusoid frequencies were all chosen to be independent integer multiples of the experiment measurement time base frequency ω_m , i.e., $\omega_t[k] = n_t[k]\omega_m$ with $\omega_m = 2\pi/T_m$. For this experiment, the experimental measurement time was $T_m = 81.92$ s, giving a base frequency of 0.0767 rad/s. The amplitudes $A_t[k]$ were chosen to give a low-pass signal characteristic approximately matching the frequency distribution of a turbulence signal²¹ and a 1.6 deg² variance for f_t over its measurement window. The phases $\phi_t[k]$ were chosen to ensure a signal of average crest factor.^{16,21} All forcing function parameters are listed in Table 1.

Table 1. Experiment target forcing function parameters.

k	n_t	ω_t , rad/s	A_t , deg	ϕ_t , rad
1	6	0.460	1.397	1.288
2	13	0.997	0.977	6.098
3	27	2.071	0.441	5.507
4	41	3.145	0.237	1.734
5	53	4.065	0.159	2.019
6	73	5.599	0.099	0.441
7	103	7.900	0.062	5.175
8	139	10.661	0.046	3.415
9	194	14.880	0.036	1.066
10	229	17.564	0.033	3.479

II.D. Experiment Conditions

In the experiment, different settings for the controlled dynamics $H_c(s)$ were tested. More specifically, to measure the noticeability and human control adaptation to changes in controlled system dynamics, the two parameters that char-

acterize the short-period mode of the aircraft pitch dynamics model of Eq. (1) – i.e., the undamped natural frequency ω_{sp} and the damping ratio ζ_{sp} – were varied with respect to their nominal values. The other two controlled system parameters, the gain K_c and the lead time constant T_{θ_2} , were kept constant at their nominal values of 0.4 and 1.0 s, respectively.

The total of 15 tested conditions (C0-C14), a factorial combination of ω_{sp} and ζ_{sp} settings, are defined in Table 2. As can be verified from Table 2, in total five settings for ω_{sp} were considered – i.e., 2, 2.5, 2.75, 3, and 3.5 rad/s – as well as ζ_{sp} settings of 0.3, 0.5, and 0.8. Note from Table 2 that the baseline condition, referred to as C0, corresponds to the baseline controlled dynamics introduced in Section II.B.

Table 2. Experimental condition definition.

Damping ratio ζ_{sp} , -	Natural frequency ω_{sp} , rad/s				
	2	2.5	2.75	3	3.5
0.3	C3	C6	C1	C9	C12
0.5	C4	C7	C0	C10	C13
0.8	C5	C8	C2	C11	C14

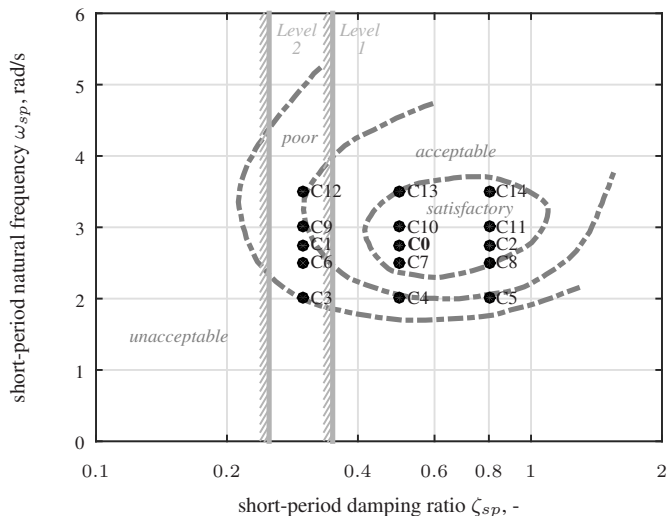


Figure 4. The thumb print criterion²⁸ with the Flight Phase Category A Level 1 and Level 2 short-period dynamic requirements from Ref. 3 and all tested experimental conditions overlaid.

Fig. 4 shows a graphical representation of the tested conditions against the *thumb print criterion*²⁸ (dashed lines) and the *Flight Phase Category A* Level 1 and Level 2 short-period dynamic requirements³ (gray boundaries). As can be verified from Fig. 4, the baseline dynamics of condition C0 meet the “satisfactory” and Level 1 requirements for both handling qualities criteria. With the tested symmetrical variations in ω_{sp} and ζ_{sp} with respect to C0, Fig. 4 shows that reduced natural frequencies and a reduced damping ratio, which results in more sluggish and less damped controlled dynamics, result in more degraded control characteristics than ω_{sp} and ζ_{sp} values that are too high. Note also that for the low short-period damping conditions with $\zeta_{sp} = 0.3$ the handling qualities are in fact Level 2 and in the “poor” region of the thumbprint criterion.

Fig. 5 shows the frequency responses of all experimental conditions, with a separate Bode plot for each ω_{sp} setting. The frequency responses of $H_c(s)$ for different ζ_{sp} are indicated with different marker colors. The baseline controlled system’s (C0) frequency response is shown in gray in all plots for reference. Finally, the MUAD envelope from Ref. 1, applied to the baseline system’s dynamics, is shown with the gray shaded area and the dashed boundaries. As any change in ω_{sp} or ζ_{sp} induces a change in $H_c(s)$ with respect to the baseline that can also be achieved by “adding” compensating dynamics to the baseline system, this MUAD envelope is used here as a reference for the expected noticeability of short-period parameter variations. Consistent with Fig. 4, Fig. 5 shows that with increased or decreased ζ_{sp} compared to the nominal setting of 0.5 $H_c(j\omega)$ is outside of the MUAD (for the magnitude), as this change in dynamics occurs where the MUAD is the most narrow. For the considered increased or decreased ω_{sp} settings, which result in changes in high-frequency gain and the position of the short-period peak, $H_c(j\omega)$ is seen to remain relatively closer to the MUAD boundaries. Hence, also Fig. 5 suggests that the considered variation in ζ_{sp} will be the most noticeable for human operators.

II.E. Apparatus

The experiment was performed in the fixed-base simulator setup of the Human-Machine Interaction Laboratory at Delft University of Technology, see Fig. 6. During the experiment the participants were seated in the right cockpit seat and a right-handed electro-hydraulic servo-controlled sidestick was used for giving pitch (fore-aft) control inputs. The roll axis of the sidestick was locked at the neutral (upright) position. The primary flight display in front of the right

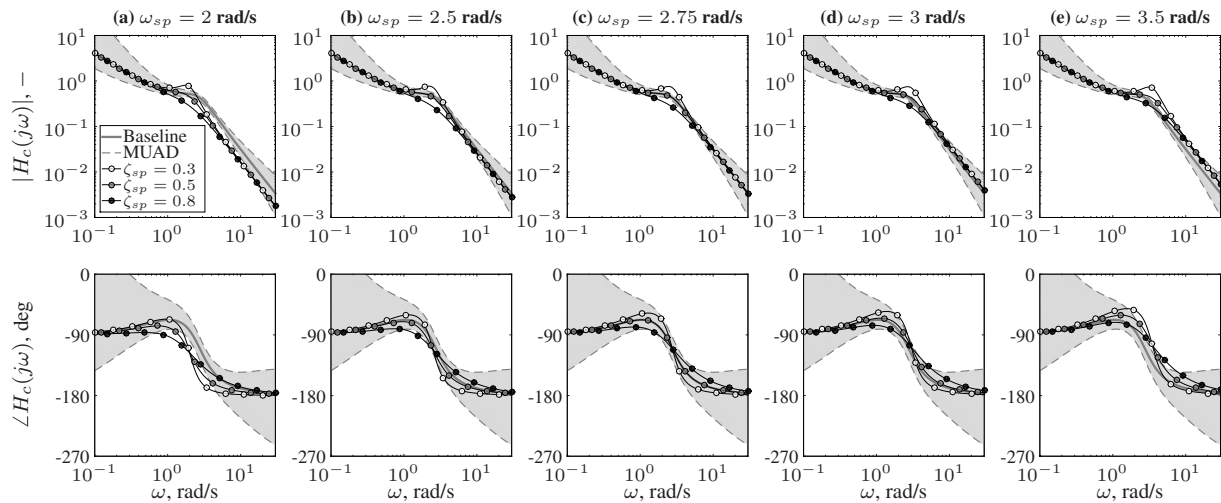


Figure 5. Frequency responses of the controlled system dynamics for all tested experimental conditions compared to the baseline dynamics and the MUAD from Ref. 1.

cockpit seat was used to present participants with the display of Fig. 2. No other visual cues were presented during the experiment, that is, the secondary flight displays and the outside visual system were switched off.



Figure 6. Fixed-base simulator setup, showing the visual display and the electro-hydraulic servo-controlled sidestick.

II.F. Participants and Experimental Procedures

Fifteen subjects were invited to perform this experiment, all MSc and PhD students or staff of the Faculty of Aerospace Engineering. All of them had prior experience with tracking tasks from previous human-in-the-loop experiments. Three participants were fixed-wing pilots with an active license. The participants were between 22 and 53 years old. Before starting the experiment the participants received a verbal briefing about the scope and objective of the experiment. The participants' were instructed to continuously try to keep the pitch tracking error as small as possible.

The experiment was performed during a single half-day session that lasted around 4 hours. The experiment had a Latin square design, see Fig. 7(a), to balance out any order effects (e.g., fatigue) over the different participants. The nominal experiment planning for participant 15 based on this Latin square design is shown in Fig. 7(b). As shown in Fig. 7(b), every participant first performed around four runs with the baseline controlled system (C0) for initial familiarization with the task. After this familiarization, participants tested the different experimental conditions in the trial order defined by the Latin square. In every trial, participants performed a nominal number of three repeated runs (R1-R3) of each condition, directly followed by a fourth run (R4) with baseline system (C0). In cases where participants required more time to adapt to a new experiment condition, 1-2 additional runs were performed. The last two runs performed for each condition, so R2 and R3 for the nominal design of Fig. 7(b), were used as the measurement data.

As indicated with the superscript numbering in Fig. 7(b), the nominal experiment consisted of 64 tracking runs. Each tracking run lasted 90 seconds. To motivate the participants to control at a consistent level of performance, they were informed of their tracking performance, expressed in terms of the root mean square of the error signal $RMS(e)$, after each run. Furthermore, during the experiment three to four breaks of around 15 minutes were taken, always in-between two trials, to limit fatigue.

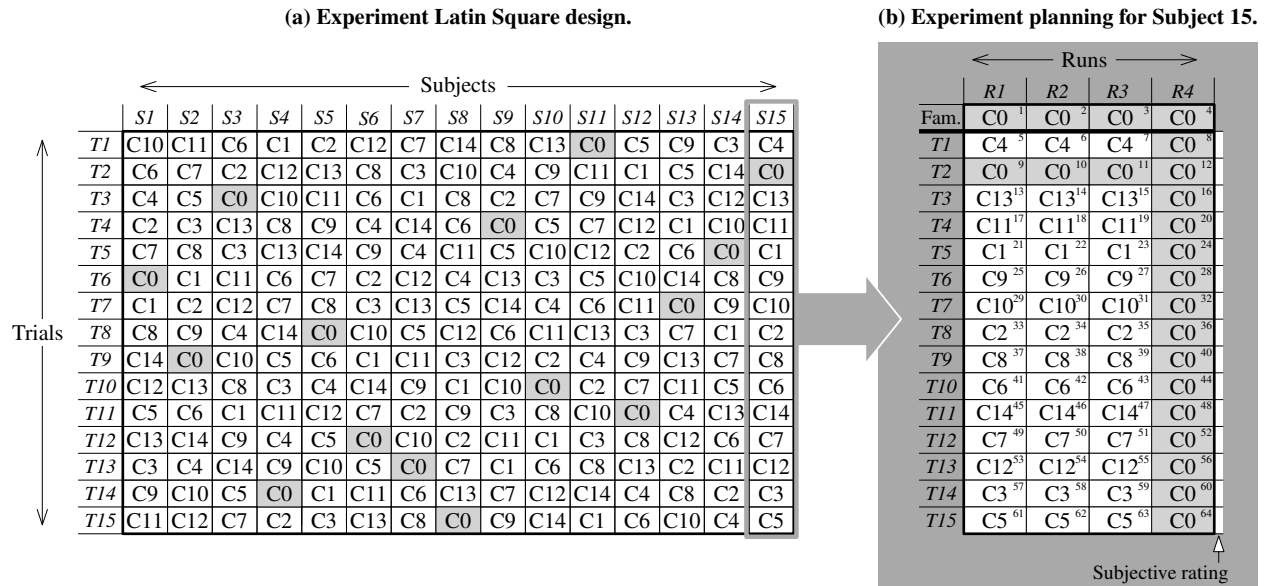


Figure 7. Latin square experiment design and nominal experiment planning for an example participant.

To also measure participants' subjective noticeability of changes in the controlled system parameter for reference, they were asked to provide a subjective rating after the final baseline run of each trial (R4 in Fig. 7(b)). Participants were asked to rate their perceived difference between the baseline dynamics (R4) and system they were controlling in the run prior to that (R3), using the rating scale of Table 3. For rating, they were asked to provide a single numeric rating ranging from 0 (no difference perceived with respect to the baseline) to 3 (experimental condition is clearly different from the baseline).

Table 3. Four-point subjective rating scale for rating the noticeability with respect to the baseline controlled system.

Rating	Interpretation
0	No difference
1	Small difference but not really noticeable
2	Noticeably different
3	Completely different

II.G. Data Analysis

II.G.1. Dependent Variables

In addition to the collected subjective rating data, objective control behavior measures were calculated from the tracking data. Each experiment run lasted 90 s, of which the final 81.92 s were used as measurement data; the first 8.08 s of data of each run were discarded. For each run the tracking error signal e and the control signal u were recorded at a frequency of 100 Hz. From these objective measurements the following dependent variables were calculated:

- $RMS(e)$: tracking performance was measured as the root mean square (RMS) of the error signal e .
- $RMS(u)$: control activity was measured as the RMS of the control input signal u .
- K_p , T_L , T_I , τ_p , ω_{nm} and ζ_{nm} : estimated human operator model parameters were used to explicitly quantify changes in participants' control behavior. For modeling the adopted control behavior, the same human operator

model as used in earlier experiments with equivalent controlled system dynamics^{21–23} was used:

$$H_p(j\omega) = K_p \frac{(T_L j\omega + 1)^2}{T_I j\omega + 1} e^{-j\omega\tau_p} H_{nm}(j\omega) \quad (3)$$

$$H_{nm}(j\omega) = \frac{1}{\frac{1}{\omega_{nm}^2}(j\omega)^2 + \frac{2\zeta_{nm}}{\omega_{nm}}j\omega + 1} \quad (4)$$

Note that the model of Eq. (3) consists of equalization dynamics and limitation terms (delay τ_p , neuromuscular dynamics $H_{nm}(j\omega)$) and is based on McRuer et al.'s *precision model*.¹⁴ To model the equalization dynamics adopted by human operators in control of systems of the form of Eq. (1) over a wide frequency range,²⁹ Eq. (3) includes a squared lead term. The six parameters of this human operator model – K_p , T_L , T_I , τ_p , ω_{nm} and ζ_{nm} – were estimated from measured time traces of e and u using the time-domain parameter estimation method described in.²⁵

II.G.2. Evaluating “Objective” Noticeability

For the experiment data, it is expected that operator adaptation to the induced changes in ω_{sp} and ζ_{sp} will be reflected by one or more of the considered dependent variables (see Section II.G.1). To be able to convert this possibly multi-variable adaptation into a single estimate of the required magnitude of operator adaptation, and thus the “noticeability” of the induced change in $H_c(s)$ from an objective behavioral analysis standpoint, in this paper we propose a straightforward procedure based on statistical differences between the data of all conditions and the baseline, C0. In this paper, we use the following parameter vector Θ_Δ that consists of a subset of all considered dependent variables for this analysis:

$$\Theta_\Delta = [\text{RMS}(e) \quad \text{RMS}(u) \quad K_p \quad T_L \quad T_I \quad \tau_p]^T \quad (5)$$

As shown by Eq. (5), Θ_Δ is chosen to consist of $\text{RMS}(e)$ and $\text{RMS}(u)$, as well as the equalization parameters (K_p , T_L , and T_I) and the response delay τ_p of the considered human operator model. The neuromuscular system parameters defined in Eq. (4) are not considered, as no structural change in these parameters is expected with varying ω_{sp} and ζ_{sp} .

To quantify the strength of a change the dependent variables in Θ_Δ compared to the baseline condition, first the mean and 95% confidence interval for C0 are calculated as the reference, i.e., μ_X^{C0} and $z_{2.5}\sigma_X^{C0}/\sqrt{n}$, respectively, with $z_{2.5}$ the 95% probability factor from the Student t distribution and n the number of samples. Furthermore, in these symbols X indicates a given dependent variable in the considered parameter vector defined in Eq. (5), i.e., $X \in \Theta_\Delta$. For any experiment condition, the difference in that condition's sample mean μ_X compared to the baseline condition mean can be calculated as:

$$\Delta\mu_X = \mu_X - \mu_X^{C0} \quad (6)$$

For rough quantification of the relevance and strength of $\Delta\mu_X$, the difference in mean is converted into logical 1 or 0, here indicated with the symbol Δ_X , based on the following decision rule:

- if $|\Delta\mu_X| > z_{2.5}\sigma_X^{C0}/\sqrt{n}$, then the considered metric for condition C* is strongly different from the corresponding baseline value, hence $\Delta_X = 1$.
- if $|\Delta\mu_X| \leq z_{2.5}\sigma_X^{C0}/\sqrt{n}$, then the considered metric for condition C* is not (statistically) different from the corresponding baseline value, hence $\Delta_X = 0$.

From the logical Δ_X that indicate for each dependent variable and condition whether a clear difference with the baseline data is present, an overall difference factor Δ is calculated for each condition as the average of Δ_X over all six parameters in Θ_Δ . For example, if for a given experiment condition only significant differences in $\text{RMS}(e)$ and K_p are found, this would give $\Delta = 2/6 = 0.33$.

As should be clear from the mathematical development, this is a practical methodology for calculating an overall “objective noticeability” metric from changes in multiple possible control behavior metrics. This approach matches similar computational steps taken in Ref. 18 and 19, but can certainly be questioned and implemented differently.

II.G.3. Data Processing and Statistics

All dependent variables were calculated for the last two tracking runs performed for each condition (R2 and R3 in Fig. 7(b)) and then averaged. The first run of each condition (R1) was discarded to eliminate any strong transitional and unsteady data due to participants' adaptation to the new controlled dynamics. These final results were analyzed with a two-way repeated-measures ANOVA for statistical effects of the short-period natural frequency (ω_{sp}) and damping ratio (ζ_{sp}) over all tested conditions. The normality of the statically compared samples was tested using a Kolmogorov-Smirnov test. Significant deviations from normality were found to only occur for 3 or less out of 15 samples for most considered dependent variables, except for T_L (5 samples) and ζ_{nm} (6 samples). Given these minor deviations from normality and the unavailability of an equivalent non-parametric two-way repeated-measures test, this paper presents regular two-way repeated-measures ANOVA for all presented metrics.

II.H. Hypotheses

For the experiment, three hypotheses were formulated based available literature regarding human control adaptation to changes in controlled dynamics' natural frequency and damping ratio¹⁵ and the correspondence of the selected conditions to the MUAD envelopes of Ref. 1 and available handling qualities criteria:^{3,28}

- H1:** With increased ω_{sp} human operators will achieve better tracking performance and have lower control activity. This is due to the added responsiveness due to both the increased bandwidth of $H_c(s)$ and the increased high-frequency gain of the controlled element. Furthermore, the operators are expected to decrease their lead time-constant to ensure that $T_L \approx 1/\omega_{sp}$. The opposite effects in all variables are expected for the corresponding decreased ω_{sp} settings.
- H2:** With increased ζ_{sp} human operators will also achieve better tracking performance, but have higher control activity. This is due to the lower short-period mode resonance peak of $H_c(s)$ and the reduced gain around ω_{sp} . This latter effect will also result in increased operator response gains K_p . The opposite effects in all variables are expected for decreased ζ_{sp} settings.
- H3:** The observed effects of ω_{sp} and ζ_{sp} are largely independent and additive, i.e., no significant interaction effects $\omega_{sp} \times \zeta_{sp}$ are expected. Overall, the considered variation ζ_{sp} will result in stronger human operator adaptation and will be more noticeable, due to the more pronounced induced changes in the dynamics of $H_c(s)$.

III. Results

III.A. Subjective Ratings

Fig. 8 shows the subjective rating data collected from the fifteen participants in the experiment. Each subplot shows a histogram of the ratings for one of the experiment conditions. Note that the subplots are ordered to match the condition definition in Table 2. In addition to the histograms, the medians M of the rating data are also indicated in Fig. 8.

Overall, Fig. 8 shows considerable spread in the rating data. Surprising is that the baseline condition (C0, Fig. 8(h)) also received mostly ratings higher than "0"; other conditions, such as C7 and C10 (see Fig. 8(g) and (i), respectively) were more often reported to not be noticeably different from the baseline controlled system than C0 itself. On average, the ratings are highest for the conditions with $\zeta_{sp} = 0.3$. Also, pairwise comparisons with C0 for all collected ratings only confirm significant differences for C1, C3, C6, C9, and C12, all conditions with $\zeta_{sp} = 0.3$. This suggests that a reduction in short-period damping was for most participants the most noticeable variation in the controlled dynamics. Also for increased short-period damping, an increase in ratings is noted, especially when also ω_{sp} was different from the baseline value of 2.75 rad/s. However, this effect, as well as any influence of varying ω_{sp} on the ratings is not evident, nor statistically significant.

III.B. Tracking Performance and Control Activity

Fig. 9 shows measured tracking error and control signal RMS data, which are here used as measures of tracking performance and control activity, respectively. In both figures, the RMS values are plotted as a function of ω_{sp} with data for ζ_{sp} settings of 0.3, 0.5, and 0.8 indicated with white, gray, and black-filled markers, respectively. The error bars indicate the 95% confidence intervals of the means, corrected for between-subject variability. For highlighting changes with respect to the data for the BL condition ($\omega_{sp} = 2.75$ rad/s, $\zeta_{sp} = 0.5$), the average and 95% confidence interval

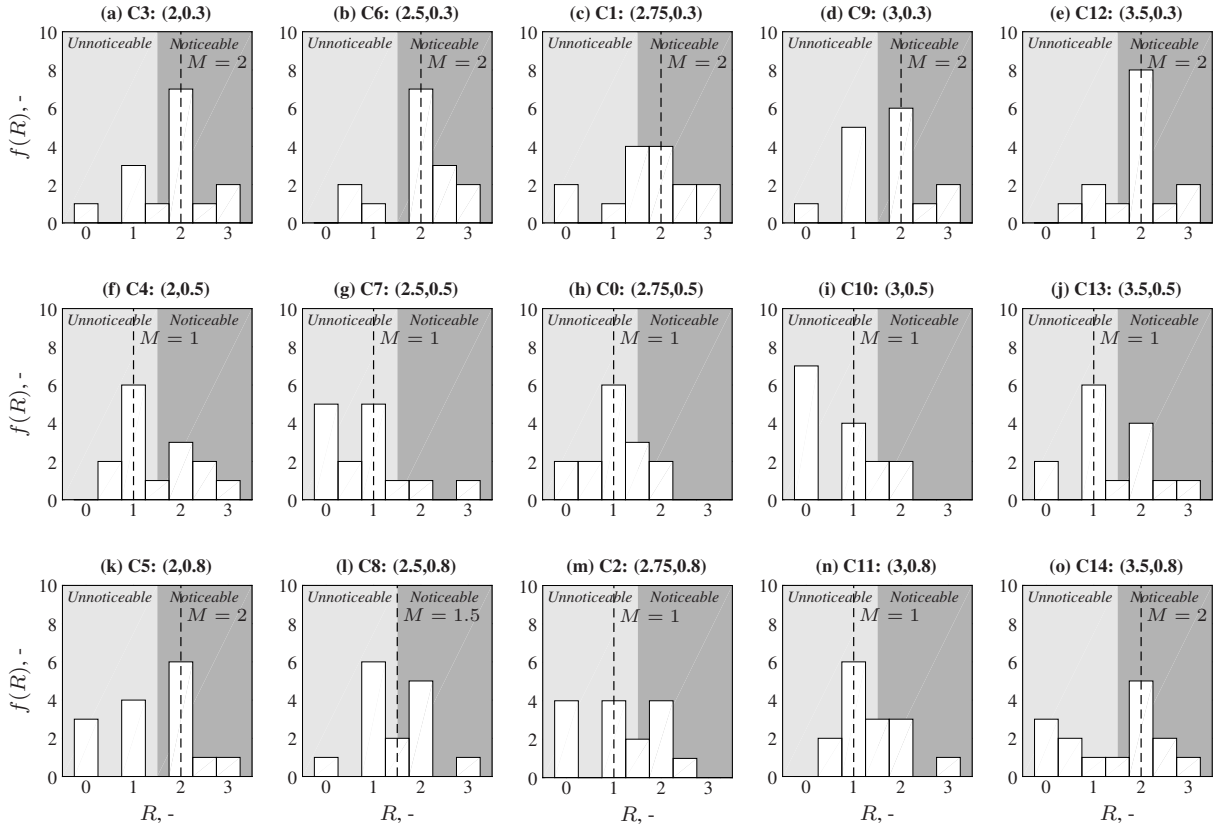


Figure 8. Histograms ($N = 15$) of subjective ratings for all experiment conditions.

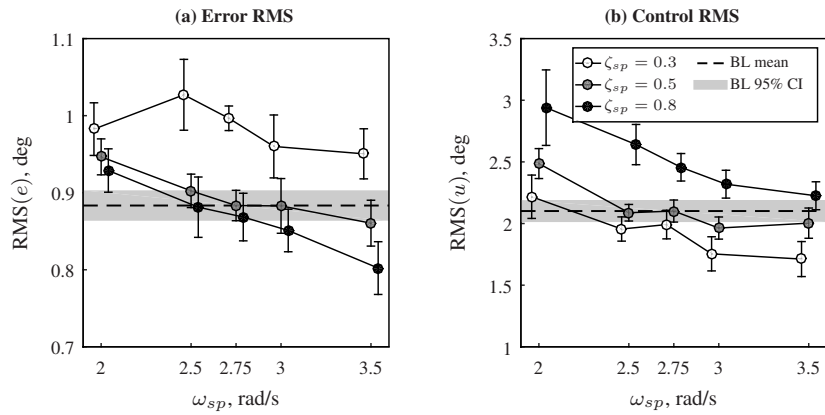


Figure 9. Measured error and control signal RMS values for all experiment conditions.

Table 4. ANOVA results for $RMS(e)$ and $RMS(u)$, where ** indicates a highly significant effect ($p < 0.01$), * indicates a significant effect ($0.01 \leq p < 0.05$), and - indicates a not significant effect ($p \leq 0.05$).

Factor	Dependent variables					
	$RMS(e)$			$RMS(u)$		
	<i>df</i>	<i>F</i>	Sig.	<i>df</i>	<i>F</i>	Sig.
ζ_{sp}	1.3,18.0 ^{gg}	47.15	**	2,28	71.77	**
ω_{sp}	4,56	14.82	**	2,2,30.1 ^{gg}	26.60	**
$\zeta_{sp} \times \omega_{sp}$	4.3,59.8 ^{gg}	2.43	-	2,9,41.1 ^{gg}	1.50	-

gg = Greenhouse-Geisser sphericity correction applied

for the baseline data are emphasized with the horizontal dashed line and the light gray shaded area, respectively. Table 4 lists the corresponding statistical analysis results for both $\text{RMS}(e)$ and $\text{RMS}(u)$.

Fig. 9(a) shows strong variations in the level of task performance due to both ζ_{sp} and ω_{sp} . Increasing the bandwidth of the controlled system (increasing ω_{sp}) is seen to result in consistently improved performance (lower $\text{RMS}(e)$). Similarly, an increased short-period damping ratio ζ_{sp} results in a further performance improvement. Compared to the baseline ζ_{sp} setting of 0.5, a reduced short-period damping ratio of 0.3 results in a 10% increase in $\text{RMS}(e)$, while an around 5% performance improvement occurs for $\zeta_{sp} = 0.8$. As can be verified from Table 4, the effects of both short-period mode parameters are found to be highly significant. Also, except for $\omega_{sp} = 2$ rad/s, where the effect of ζ_{sp} is found to be notably less strong than for higher short-period natural frequency settings, the effects of ζ_{sp} and ω_{sp} on $\text{RMS}(e)$ are found to be independent and no significant interaction effect between both parameters is found (see Table 4).

For the control signal RMS, Fig. 9(b) shows effects of ζ_{sp} and ω_{sp} that are highly similar to those observed for $\text{RMS}(e)$. Control effort is seen to consistently decrease (lower $\text{RMS}(u)$) with both increasing short-period frequencies (higher ω_{sp}) and decreasing short-period damping (lower ζ_{sp}). As also found for the error RMS, the variation in $\text{RMS}(u)$ over the tested range of ζ_{sp} is larger than induced by varying ω_{sp} . Again, both these effects of ζ_{sp} and ω_{sp} are highly significant, see Table 4, and no evidence for an interaction effect between both factors is found.

As can be verified from Fig. 9, tracking performance and control activity are both highly sensitive to changes in the control system's parameters. Only for very small changes in ω_{sp} the measured values for $\text{RMS}(e)$ and $\text{RMS}(u)$ are seen to still fall within the confidence intervals of the BL data. While statistical differences in these parameters by no means equate to noticeability, consistent differences in error and control above a certain magnitude will certainly become noticeable.

III.C. Human Operator Model Parameters

Fig. 10 shows example human operator modeling results for a single participant (Subject 2) and a subset of all tested experiment conditions. For all other participants and conditions equivalent results were obtained, but are not presented here for brevity. Compared to the baseline condition (C0, Fig. 10(c)), Fig. 10(b) and (d) illustrate the changes in operator control dynamics over the range of tested ω_{sp} settings, keeping ζ_{sp} constant. Fig. 10(a) and (e) then show the further control adaptations due to reduced or increased short-period damping for conditions C3 and C14, respectively.

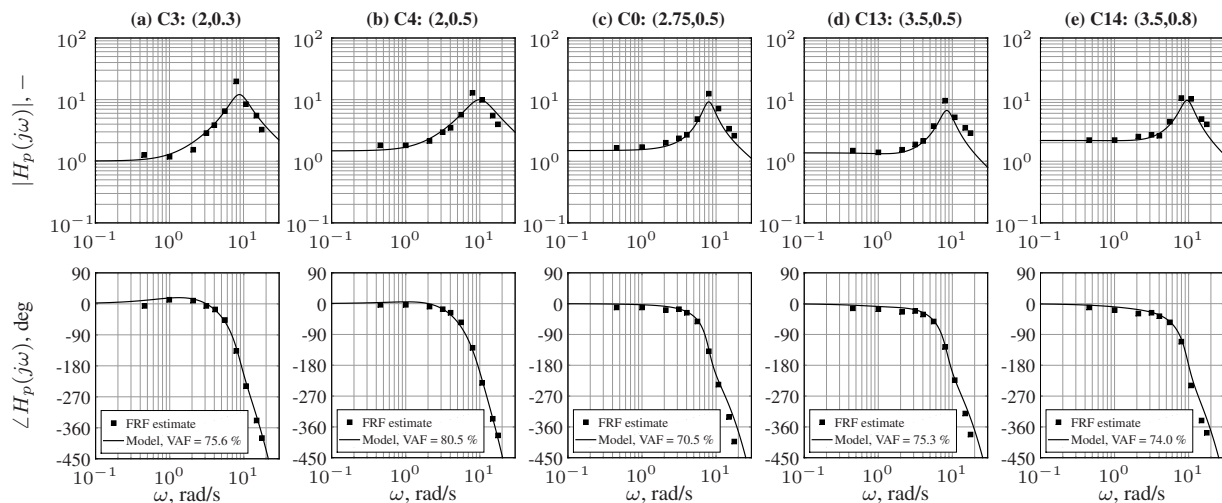


Figure 10. Estimated human operator frequency responses and fitted models for Subject 2, conditions C3, C4, C0, C13, and C14.

Overall, Fig. 10 shows that the assumed human operator model of Eq. (3) accurately captures the measured control behavior over the full range of variations in ω_{sp} and ζ_{sp} . For all participants and conditions human operator model VAF values of around 70% or higher were obtained, with no consistent variation in VAF over conditions. Furthermore, the frequency response data in Fig. 10 also illustrates some of the main behavioral adjustments with the applied variation in ω_{sp} and ζ_{sp} . Decreased ω_{sp} compared to the baseline setting (see Fig. 10(a) and (b)) is seen to result in increased operator lead equalization, as evidenced from the increased positive slope of $|H_p(j\omega)|$ and the increase in $\angle H_p(j\omega)$ at mid frequencies. In addition, compared to C0, the low-frequency magnitude of $H_p(j\omega)$ is seen to decrease for C3 ($\zeta_{sp} = 0.3$) and increase for C14 ($\zeta_{sp} = 0.8$), as expected for the tested variation in short-period damping ratio.

Fig. 11 shows the average estimated human operator model parameter results in the same format as used for the tracking performance and control activity data in Fig. 9. Note that the presented error bars indicate the 95% confidence intervals of the means over all subjects that these have been corrected for between-subject variability. The corresponding statistical analysis results are presented in Table 5 and 6. Overall, the human operator model defined by Eqs. (3) and (4) was found to accurately describe the measured data, with an average Variance Accounted For (VAF) of 78.4% for the baseline condition and an average VAF of 77.9% over all other conditions.

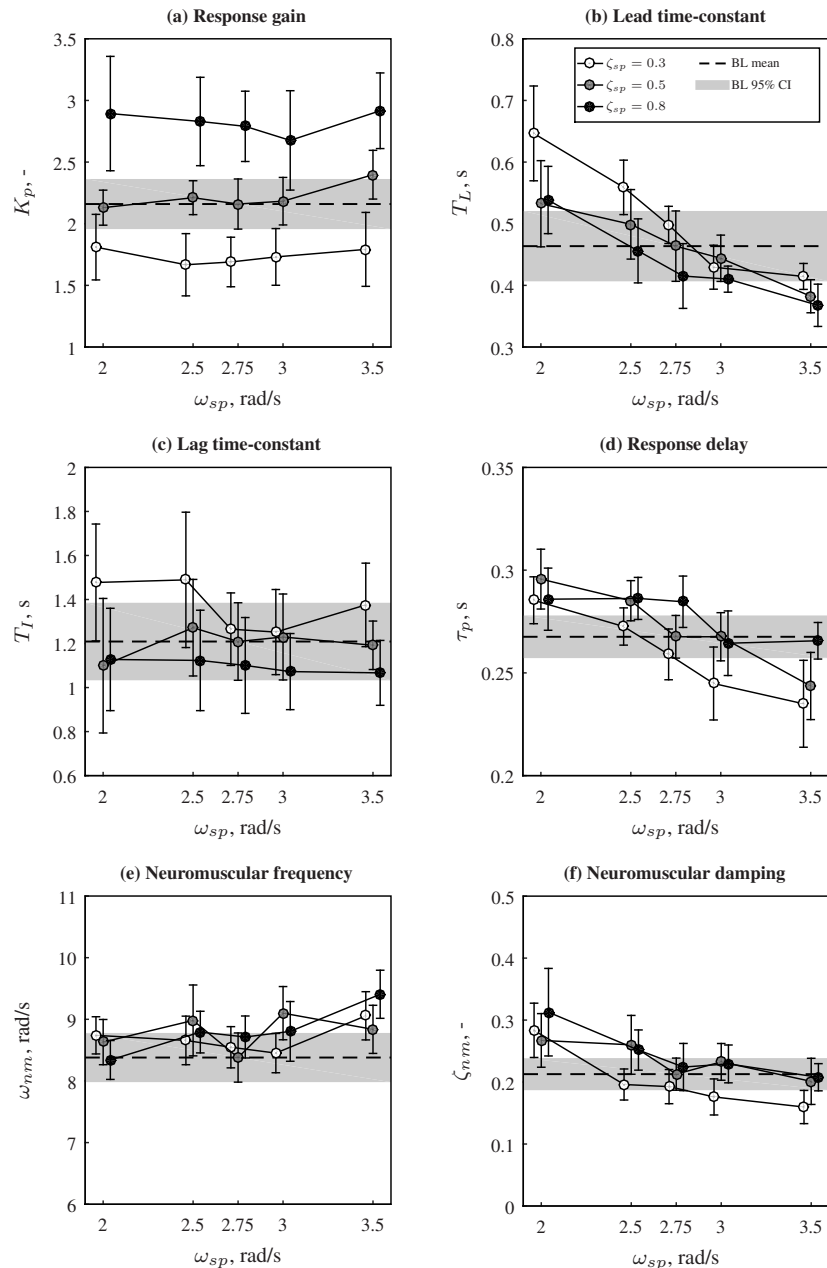


Figure 11. Estimated human operator model parameters for all experiment conditions.

Fig. 11 shows clear and consistent adaptation of human operators' control dynamics to the applied variations in ζ_{sp} and ω_{sp} . As expected (Hypothesis H2), changes in short-period damping result in a notable adjustment of human operators' response gain K_p , see Fig. 11(a). With increased damping ($\zeta_{sp} = 0.8$), K_p is more than 20% higher than for the baseline setting, while for $\zeta_{sp} = 0.3$ a reduction in K_p of around 20% is observed. The lag-time constant T_I , see Fig. 11(c), shows a similar (yet opposite) variation with ζ_{sp} : for reduced ζ_{sp} a consistent increase in T_I is observed, which results in a further reduction of the human operator magnitude at low frequencies, while a consistent reduction in the lag time-constant is found for $\zeta_{sp} = 0.8$. As can be verified from Table 5, both the effects of ζ_{sp}

Table 5. ANOVA results for the estimated human operator model parameters, where ** indicates a highly significant effect ($p < 0.01$), * indicates a significant effect ($0.01 \leq p < 0.05$), and - indicates a not significant effect ($p \leq 0.05$).

Factor	Dependent variables											
	K_p			T_L			T_I			τ_p		
	df	F	Sig.	df	F	Sig.	df	F	Sig.	df	F	Sig.
ζ_{sp}	1.1,15.9 ^{gg}	31.05	**	2,28	12.42	**	2,28	7.38	**	2,28	7.30	**
ω_{sp}	2.5,35.2 ^{gg}	1.02	-	4,56	27.99	**	2,4,33.7 ^{gg}	0.48	-	2,7,37.1 ^{gg}	21.42	**
$\zeta_{sp} \times \omega_{sp}$	8,112	0.39	-	4,3,60.7 ^{gg}	1.32	-	8,112	0.61	-	8,112	1.42	-

gg = Greenhouse-Geisser sphericity correction applied

Table 6. ANOVA results of pilot neuromuscular parameters, where ** indicates a highly significant effect ($p < 0.01$), * indicates a significant effect ($0.01 \leq p < 0.05$), and - indicates a not significant effect ($p \leq 0.05$).

Factor	Dependent variables					
	ω_{nm}			ζ_{nm}		
	df	F	Sig.	df	F	Sig.
ζ_{sp}	2,28	0.62	-	2,28	13.65	**
ω_{sp}	4,56	4.17	**	4,56	4.08	**
$\zeta_{sp} \times \omega_{sp}$	8,112	1.82	-	8,112	1.30	-

on K_p and T_I are statistically significant. In addition to these effects on the (low-frequency) human control gain, ζ_{sp} variations also significantly affect other human operator model parameters. For example, Fig. 11(b) shows that the lead time-constant T_L increases with reduced short-period damping ($F(2, 28) = 12.4$, $p < 0.01$), especially for low ω_{sp} . In addition, both the response delay τ_p and neuromuscular damping ratio ζ_{nm} – see Fig. 11(d) and (f), respectively – show a significant decrease with decreasing ζ_{sp} (Tables 5 and 6).

With changes in the short-period natural frequency ω_{sp} , human operators were expected to adapt their lead time-constant to achieve $T_L \approx 1/\omega_{sp}$. As can be verified from Fig. 11(b), this change in T_L is indeed observed from the estimated human operator parameter values and statistically significant, $F(4, 56) = 28.0$, $p < 0.01$. With the increased lead-equalization adopted for decreasing ω_{sp} , human operators are also found to significantly increase their response delay τ_p (Fig. 11(d)) and neuromuscular damping ratio (Fig. 11(f)), see Tables 5 and 6. Finally, Fig. 11(e) also shows that human operators consistently increase their neuromuscular system natural frequency ω_{nm} with around 0.5 rad/s for the high short-period frequency setting $\omega_{sp} = 3.5$ rad/s, another significant effect, $F(4, 56) = 4.2$, $p < 0.01$, see Table 6.

As can be verified from Fig. 11, in spite of the significant effects of ζ_{sp} and ω_{sp} on the human operator model parameters, in many cases the measured average values are seen to still fall within the 95% confidence bounds of the BL data. Especially for C7 and C10, which only have a small deviation in ω_{sp} from the baseline dynamics, most parameters show only very minor differences with the BL data. Finally, as expected (Hypothesis 3), Fig. 11 and Tables 5 and 6 also show no evidence of interaction effects between the applied variations in ζ_{sp} and ω_{sp} , which confirms that human adaptation to changes in these parameters is largely independent and additive.

III.D. Objective and Subjective Noticeability Comparison

Traditionally, MUAD¹ and Allowable Error⁴ envelopes have been developed based on subjective pilot rating data. To verify to what extent such envelopes could potentially also be derived from objective human operator control metrics, Fig. 12 shows a direct comparison of the overall objectively measured change in manual control performance and dynamics against the subjective ratings awarded in the current experiment. Fig. 12 shows the median of the collected subjective ratings $M(R)$, see Fig. 8, plotted against the values of the objective “noticeability” parameter Δ calculated from the objective control behavioral parameter data of Figs. 9 and 11 as described in Section II.G.2. In addition, Fig. 12 shows a clustering of the data for the tested experiment conditions, indicated with the gray and hatched areas.

Fig. 12 shows indications of a correlation between the objectively measured changes in human operator behavior and the median subjective ratings that is also consistent with the comparison of all tested conditions with available handling qualities criteria and MUAD envelopes in Section II.B. For example, the lowest $M(R)$ and Δ values are found for the baseline condition C0 and the two conditions with the same ζ_{sp} as C0 and a small 0.25 rad/s difference in ω_{sp} (C7 and C10). As can be verified from Fig. 5, C7 and C10 are also the only tested conditions for which the change in $H_c(s)$ remains within the MUAD envelope of Ref. 1.

As shown in Fig. 12, the highest $M(R)$ and Δ are found for two subsets of conditions. First, all conditions with a reduced short-period damping ratio $\zeta_{sp} = 0.3$ (i.e., C1, C3, C6, C9, and C12) were awarded a median rating of 2 and showed behavioral adaptation in 50-100% of the considered dependent variables. This is expected given Fig. 4, as the reduced ζ_{sp} meant a drop to Level 2 handling qualities and the “poor” region of the Thumbprint criterion. The second

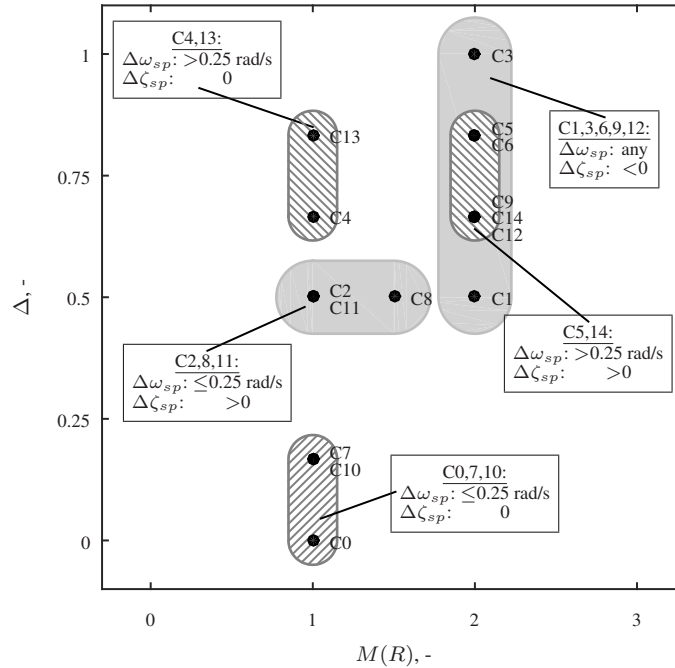


Figure 12. Comparison of the objective “noticeability” parameter Δ with the median of the collected rating data $M(R)$.

subset for which high $M(R)$ and Δ were found are conditions C5 and C14, which both have increased short-period damping and large changes in ω_{sp} compared to the baseline.

For the remaining conditions, i.e., those with only changes in ω_{sp} larger than 0.25 rad/s (C4 and C13) or small changes in ω_{sp} combined with an increased short-period damping ratio of $\zeta_{sp} = 0.8$ (C2, C8, and C11), Fig. 12 shows that significant differences were observed in multiple objective behavioral parameters ($\Delta \geq 0.5$), but mostly $M(R) = 1$ are obtained from the subjective ratings. Especially comparing conditions C4 and C13 with conditions C5 and C14 in Fig. 12, this suggests that the induced adaptation of manual control behavior with changes in $H_c(s)$, though considerable from an objective metric standpoint, is not always consistently subjectively perceived.

Finally, reflecting on the calculation of the objective “noticeability” parameter Δ with the procedure described in Section II.G.2 from the experiment data presented in Fig. 9 and 11, it is clear that not all parameters assumed in Θ_Δ show equally strong variations over the tested experiment conditions. The most sensitive dependent variables, i.e., those that most often differed significantly from their values for condition C0, were found to be $RMS(u)$ (87%), K_p (73%), $RMS(e)$ (67%), and τ_p (60%). With comparatively smaller variations and larger spread, the lead and lag time-constants contributed less often to Δ , i.e., for 40% and 13% of the tested conditions.

IV. Discussion

A human-in-the-loop experiment was performed to explicitly measure human operators’ sensitivity, based on objective control-behavioral analysis, to induced changes in the short-period natural frequency and damping ratio. The main goal of the experiment was to contribute to the on-going development of objective “manual control adaptation” envelopes¹⁸ that quantify the maximum allowable variations in controlled dynamics that do not induce a change in human control behavior. The experiment used a nominal low-order aircraft model representative for a Cessna Citation aircraft as the baseline and tested five different ω_{sp} and three different ζ_{sp} settings centered around this baseline. Objective control behavior metrics (e.g., tracking performance, control activity, and estimated human operator model parameters) were used to compare human adaptation over the different tested conditions. Furthermore, a new methodology was proposed to derive an overall “objective noticeability” parameter from these typically considered control behavior metrics, which was also correlated with the subjective noticeability ratings collected in the experiment.

Three hypothesis were formulated for the experiment and, based on the collected experiment data, all three are accepted. As expected from **Hypothesis H1**, a higher short-period natural frequency ω_{sp} was found to result in significantly better performance (lower $RMS(e)$), reduced control activity (lower $RMS(u)$), and lower lead-time constants

T_L , while the matching opposite effects were observed for ω_{sp} settings lower than the baseline value. In addition to these expected effects, human operators were found to significantly change their response delay τ_p and neuromuscular dynamics with varying ω_{sp} . Response delays were up to 60 ms lower when controlling aircraft dynamics with $\omega_{sp} = 3.5$ rad/s than with 2 rad/s, which is consistent with the reduced need for lead equalization.¹⁵ With increasing ω_{sp} , the neuromuscular frequency ω_{nm} and damping ratio ζ_{nm} were found to significantly increase and decrease, respectively. Both effects are relatively small in magnitude, but still indicate more tight control with high ω_{sp} .

As defined in **Hypothesis H2**, better short-period damping (increased ζ_{sp}) was expected to improve tracking performance and result in increased control activity and operator response gains K_p , while the opposite effects were expected for reduced ζ_{sp} . For $\text{RMS}(e)$, $\text{RMS}(u)$, and K_p indeed very strong and significant effects of ζ_{sp} are found, e.g., measured human operator response gains are two times as high for $\zeta_{sp} = 0.8$ as for $\zeta_{sp} = 0.3$. In addition, also all other considered human operator model parameters except for ω_{nm} show more minor, yet still statistically significant, variations over the different tested ζ_{sp} settings. Both the lead (T_L) and lag (T_I) time-constants are found to be consistently higher with reduced ζ_{sp} , indicating increased lead equalization, while human operator response delays are on average slightly reduced. Overall, these adaptations are consistent with how human operators would need to adapt to the more difficult task for $\zeta_{sp} = 0.3$, i.e., controlling an aircraft with degraded (Level 2) handling qualities.

Finally, we expected (**Hypothesis H3**) the effects of ω_{sp} and ζ_{sp} on human operator behavior and performance to be largely independent and additive. Indeed, none of the considered dependent variables show evidence of an interaction between both short-period parameters, which is confirmed by the performed statistical analysis, i.e., no significant interaction effects $\omega_{sp} \times \zeta_{sp}$ were found. Overall, as also expected from comparison of the tested $H_c(s)$ settings with available handling qualities criteria^{3,28} and MUAD envelopes,¹ the results confirm that the considered variations in ζ_{sp} lead to stronger human operator adaptation. Also the collected subjective rating data confirms this, as the conditions with $\zeta_{sp} = 0.8$ and especially $\zeta_{sp} = 0.3$ were more frequently rated as “noticeably different” from the baseline, than the conditions with only a different ω_{sp} setting.

In this paper we proposed a novel, rudimentary, methodology to estimate the overall “objective noticeability” of variations in the controlled dynamics from the objectively measured changes in human operators’ manual control performance and behavior. For this, it was proposed to convert the *multi*-variable adaptation measured from all considered dependent variables into a *single* estimate of the overall adaptation, by checking for statistically significant differences (i.e., yes/no) between the data of each condition and the baseline. The final “objective noticeability” parameter Δ was then calculated as the percentage of considered dependent variables (here chosen as $\text{RMS}(e)$, $\text{RMS}(u)$, and all human operator model parameters except ω_{nm} and ζ_{nm}) for which a significant difference with the baseline data was present. Overall, the proposed Δ parameter seems to consistently capture and quantify the overall objective adaptation of human operators’ manual control behavior to variations in short-period damping ratio and natural frequency. Furthermore, it also correlates well with the subjective noticeability ratings collected in the experiment (e.g., effects of ζ_{sp}), which warrants the further development of objective “manual control adaptation” envelopes based on such an “objective noticeability” parameter, to augment currently available MUAD¹ and AE⁴ envelopes that are defined from subjective rating data.

The further development of the proposed methodology towards the definition of objective “manual control adaptation” envelopes, as also proposed in Ref. 18, requires further investigation of some of the key assumptions made in calculating Δ . Especially the selection of dependent variables considered in the calculation of Δ , in this paper represented by the parameter vector Θ_Δ , represents a critical choice. For example, in this paper Δ was calculated based on a selected set of dependent variables for which an induced change due to ω_{sp} and ζ_{sp} variations was expected, which excluded the neuromuscular system parameters of the considered human operator model. However, as especially ζ_{nm} did in fact show statistically significant adaptation to both short-period parameters for the collected experiment data, it should perhaps be considered as an additional indicator in Θ_Δ . On the other hand, in the definition of Θ_Δ also the potential (and likely) correlations between the different dependent variables – e.g., in general higher K_p results in better performance and thus lower $\text{RMS}(e)$ ¹⁵ – should be accounted for, to ensure that strong inherently linked and “overlapping” parameter changes do not completely dominate the calculation of Δ .

The current experiment collected manual control data for a comparatively high number of different controlled aircraft dynamics settings, i.e., fifteen different combinations of ω_{sp} and ζ_{sp} . For the chosen experiment setup, this resulted in an experiment that could feasibly be performed in a single half-day experiment session. Looking at the resulting experiment data, it is clear that despite the high number of tested conditions more data is needed to fully grasp human control adaptation to ω_{sp} and ζ_{sp} . For example, for both parameters only a relatively small range of values is tested. For example, the considered ω_{sp} settings do not cover aircraft dynamics with poor handling qualities. In addition, especially for ζ_{sp} , only a very coarse “grid” of values is tested, leading to limited insight in the true trend of adaptations to ζ_{sp} . However, as we will always remain limited in the number of conditions that can be feasibly

tested in human-in-the-loop experiments, a viable approach to increase the data density for this application may be to augment experiment datasets with simulated predictions of control behavior adaptation. Recent efforts have shown that behavioral adaptations to *added* dynamics in $H_c(s)$ are accurately predicted from offline simulations.^{18,19} As human adaptation to changes in the aircraft dynamics parameters, as considered here, is not fundamentally different from adaptation to added dynamics, we expect the same success for offline prediction of the effects of ω_{sp} and ζ_{sp} .

Finally, the current experiment was setup to collect accurate objective data of human control adaptation to (a large number of) different controlled aircraft dynamics settings. This deliberate focus has also directly impacted the reliability of the subjective noticeability ratings that were collected in the experiment, for reference. Verifying the current objective behavioral findings with accurate subjective data requires a completely different experiment setup. For example, more accurate subjective data can be collected based on pairwise comparisons between the baseline dynamics and aircraft dynamics with modified short-period parameters in two consecutive and shorter (e.g., 10 seconds) tracking segments. Using adaptive staircase procedures as also successfully applied for measuring perceptual thresholds,^{30,31} the subjective noticeability of changes in the controlled dynamics can then be accurately measured.

V. Conclusion

In this paper, an experiment with 15 participants performed to investigate human operators' sensitivity to variations in the short-period mode characteristics of the controlled aircraft dynamics in a pitch tracking task is described. In the experiment, objective human control data and subjective noticeability ratings were collected for fifteen different tested aircraft dynamics configurations, i.e., the factorial variation of three settings for the short-period damping ratio (0.3, 0.5, and 0.8) and five short-period natural frequencies (2.0, 2.5, 2.75, 3.0, and 3.5 rad/s). Compared to the baseline controlled element with $\zeta_{sp} = 0.5$ and $\omega_{sp} = 2.75$ rad/s, which matched the low-order approximation of a Cessna Citation's pitch dynamics considered in a number of earlier experiments, adaptation of manual control behavior was measured with metrics of task performance, control activity, and estimated human operator model parameters. Overall, the current experiment shows that manual control behavior, task performance, and control activity are all highly sensitive to changes in the controlled system's short-period parameters. Human operators mainly adapt to changes in ζ_{sp} by adjusting their control gain, while ω_{sp} variations were found to lead to significant adjustments of operators' lead time-constants, neuromuscular damping ratios, and response delays. It was found that only for very small changes in ω_{sp} and ζ_{sp} the measured values for the considered behavioral metrics still fell within the confidence intervals of the baseline condition data. The novel computational approach proposed to quantify the *overall* extent of manual control adaptation to changes in ω_{sp} and ζ_{sp} from these possible changes in *many individual* dependent variables (e.g., $RMS(e)$, $RMS(u)$, and human operator model parameters) showed very good correlation with both the subjective data and available handling qualities and MUAD criteria. Thus, this approach shows potential for the development of objective "manual control adaptation" envelopes that quantify the maximum allowable changes in controlled dynamics that do not induce a change in human control behavior, as an alternative to the available envelopes developed based on subjective noticeability.

Acknowledgments

The authors would like to thank the NITROS ("Network for Innovative Training on ROTocraft Safety") project for supporting the first author's conference attendance and presentation of this conference paper. The NITROS project has received funding from the European Union's Horizon 2020 research and innovation program under the Marie Skłodowska-Curie grant agreement No. 721920.

References

- ¹Wood, J. R. and Hodgkinson, J., "Definition of Acceptable Levels of Mismatch for Equivalent Systems of Augmented CTOL Aircraft," Tech. Rep. MDC A6792, McDonnell Aircraft Company, St. Louis (MO), Dec. 1980.
- ²Carpenter, C. G. and Hodgkinson, J., "V/STOL Equivalent Systems Analysis," Tech. Rep. NADC-79141-60, United States Navy, Naval Air Development Center, Warminster, Pennsylvania 18974, May 1980.
- ³Anonymous, "Flying Qualities of Piloted Aircraft," Department of Defense Handbook MIL-HDBK-1797, Department of Defense, United States of America, Dec. 1997.
- ⁴Mitchell, D. G., Hoh, R. H., He, C., and Strobe, K., "Determination of Maximum Unnoticeable Added Dynamics," *Proceedings of the AIAA Atmospheric Flight Mechanics Conference and Exhibit, Keystone (CO)*, No. AIAA-2006-6492, 2006.
- ⁵Ashkenas, I. L. and McRuer, D. T., "A Theory of Handling Qualities Derived from Pilot-Vehicle System Considerations," *Aerospace Engineering*, Vol. 21, No. 2, 1962, pp. 60–102.

⁶Neal, T. P. and Smith, R. E., "A Flying Qualities Criterion for the Design of Fighter Flight-Control Systems," *Journal of Aircraft*, Vol. 8, No. 10, Oct. 1971, pp. 803–809.

⁷Hodgkinson, J., "History of Low-Order Equivalent Systems for Aircraft Flying Qualities," *Journal of Guidance, Control, and Dynamics*, Vol. 28, No. 4, July-August 2005, pp. 577–583.

⁸Bosworth, J. T. and Williams-Hayes, P. S., "Flight Test Results from the NF-15B Intelligent Flight Control System (IFCS) Project with Adaptation to a Simulated Stabilator Failure," *Proceedings of the AIAA InfotechAerospace 2007 Conference and Exhibit, Rohnert Park (CA)*, No. AIAA-2007-2818, 2007.

⁹Geluardi, S., Nieuwenhuizen, F. M., Pollini, L., and Bühlhoff, H. H., "Frequency Domain System Identification of a Light Helicopter in Hover," *Proceedings of the AHS 70th Annual Forum, Montreal, Canada*, 2014.

¹⁰Tischler, M. B., "System Identification Methods for Aircraft Flight Control Development and Validation," NASA Technical Memorandum 110369, NASA Ames Research Center, Moffett Field (CA), Oct. 1995.

¹¹Field, E. J., Rossitto, K. F., and Hodgkinson, J., "Identification of Frequency Responses from Flight Data and Their Application for Flying Qualities Analyses," *Proceedings of the AIAA Atmospheric Flight Mechanics Conference and Exhibit, Austin (TX)*, No. AIAA-2003-5537, 2003.

¹²Cotting, M. C., "Applicability of Human Flying Qualities Requirements for UAVs, Finding A Way Forward," *Proceedings of the AIAA Atmospheric Flight Mechanics Conference, Chicago (IL)*, No. AIAA-2009-6322, 2009.

¹³Mitchell, D. G., Nicoll, T. K., Klyde, D. H., and Schulze, P. C., "Effects of Time-Varying Rotorcraft Dynamics on Pilot Control," *Proceedings of the AIAA Atmospheric Flight Mechanics Conference, Chicago (IL)*, No. AIAA-2009-6055, 2009.

¹⁴McRuer, D. T., Graham, D., Krendel, E. S., and Reisener, W. J., "Human Pilot Dynamics in Compensatory Systems, Theory Models and Experiments with Controlled Element and Forcing Function Variations," Tech. Rep. AFFDL-TR-65-15, Air Force Flight Dynamics Laboratory, Wright-Patterson Air Force Base (OH), 1965.

¹⁵McRuer, D. T. and Jex, H. R., "A Review of Quasi-Linear Pilot Models," *IEEE Transactions on Human Factors in Electronics*, Vol. HFE-8, No. 3, Sept. 1967, pp. 231–249.

¹⁶Damveld, H. J., van Paassen, M. M., and Mulder, M., "Cybernetic Approach to Assess Aircraft Handling Qualities," *Journal of Guidance, Control, and Dynamics*, Vol. 34, No. 6, Nov.-Dec. 2011, pp. 1886–1898.

¹⁷Mulder, M., Pool, D. M., Abbink, D. A., Boer, E. R., Zaal, P. M. T., Drop, F. M., van der El, K., and van Paassen, M. M., "Manual Control Cybernetics: State-of-the-Art and Current Trends," *IEEE Transactions on Human-Machine Systems*, 2017.

¹⁸Lu, T., *Objective Evaluation of Human Manual Control Adaptation Boundaries using a Cybernetic Approach*, Ph.D. thesis, Delft University of Technology, Faculty of Aerospace Engineering, April 2018.

¹⁹Lu, T., Pool, D. M., van Paassen, M. M., and Mulder, M., "Quantifying the Effects of Added Dynamics with Human Operator Control Behavior Measurements and Simulations," *Proceedings of the AIAA Modeling and Simulation Technologies Conference, Denver (CO)*, No. AIAA-2017-3667, 2017.

²⁰Matamoros, I., Lu, T., van Paassen, M. M., and Pool, D. M., "A Cybernetic Analysis of Maximum Unnoticeable Added Dynamics for Different Baseline Controlled Systems," *Proceedings of the the 20th IFAC World Congress, Toulouse, France*, July 2017, pp. 16417–16422.

²¹Zaal, P. M. T., Pool, D. M., de Bruin, J., Mulder, M., and van Paassen, M. M., "Use of Pitch and Heave Motion Cues in a Pitch Control Task," *Journal of Guidance, Control, and Dynamics*, Vol. 32, No. 2, 2009, pp. 366–377.

²²Pool, D. M., Zaal, P. M. T., van Paassen, M. M., and Mulder, M., "Effects of Heave Washout Settings in Aircraft Pitch Disturbance Rejection," *Journal of Guidance, Control, and Dynamics*, Vol. 33, No. 1, 2010, pp. 29–41.

²³Pool, D. M., Harder, G. A., and van Paassen, M. M., "Effects of Simulator Motion Feedback on Training of Skill-Based Control Behavior," *Journal of Guidance, Control, and Dynamics*, Vol. 39, No. 4, 2016, pp. 889–902.

²⁴Zaal, P. M. T., Pool, D. M., van Paassen, M. M., and Mulder, M., "Comparing Multimodal Pilot Pitch Control Behavior Between Simulated and Real Flight," *Journal of Guidance, Control, and Dynamics*, Vol. 35, No. 5, September-October 2012, pp. 1456–1471.

²⁵Zaal, P. M. T., Pool, D. M., Chu, Q. P., van Paassen, M. M., Mulder, M., and Mulder, J. A., "Modeling Human Multimodal Perception and Control Using Genetic Maximum Likelihood Estimation," *Journal of Guidance, Control, and Dynamics*, Vol. 32, No. 4, 2009, pp. 1089–1099.

²⁶Bryan, G. H., *Stability in Aviation. An Introduction to Dynamical Stability as Applied to the Motion of Aeroplanes*, Macmillan and Co., Ltd., St. Martin's Street, London, 1911.

²⁷Hall, I. A. M., "Study of the Human Pilot as a Servo Element," *Journal of the Royal Aeronautical Society*, Vol. 67, 1963, pp. 351–360.

²⁸Chalk, C. R., "Additional Flight Evaluations of Various Longitudinal Handling Qualities in a Variable-Stability Jet Fighter," Tech. Rep. WADC-TR 57-719, Wright Air Development Center, 1958.

²⁹Pool, D. M., Zaal, P. M. T., Damveld, H. J., van Paassen, M. M., van der Vaart, J. C., and Mulder, M., "Modeling Wide-Frequency-Range Pilot Equalization for Control of Aircraft Pitch Dynamics," *Journal of Guidance, Control, and Dynamics*, Vol. 34, No. 5, September-October 2011, pp. 1529–1542.

³⁰Beckers, N. W. M., Pool, D. M., Valente Pais, A. R., van Paassen, M. M., and Mulder, M., "Perception and Behavioral Phase Coherence Zones in Passive and Active Control Tasks in Yaw," *Proceedings of the AIAA Modeling and Simulation Technologies Conference 2012, Minneapolis (MN)*, No. AIAA-2012-4794, 2012.

³¹Fu, W., van Paassen, M. M., and Mulder, M., "The Influence of Discrimination Strategy on the JND in Human Haptic Perception of Manipulator Stiffness," *AIAA Modeling and Simulation Technologies Conference*, No. AIAA-2017-3668, 2017.